Joint Torque Control for Backlash Compensation in Two-Inertia System

Shota Yamada*, Hiroshi Fujimoto**
The University of Tokyo
5-1-5, Kashiwanoha, Kashiwa, Chiba, 227-8561 Japan
Phone: +81-4-7136-3873*, +81-4-7136-4131**
Email: yamada@hflab.k.u-tokyo.ac.jp, fujimoto@k.u-tokyo.ac.jp

Yuki Terada
DMG MORI SEIKI CO., LTD.
362, Idono, Yamatokoriyama, Nara, 639-1183 Japan
Phone: +81-743-53-1122
Email: yk-terada@dmgmori.co.jp

***Abstract*—In controlling ball-screw driven stages of machine tools, industrial robots, and welfare robots, they are modelled as two-inertia systems to consider their transmission characteristics such as low rigidity and nonlinearity. To obtain precise position at the load side, the number of devices with load-side encoders is increasing. The precise joint torque control method and the load-side torque control method for a two-inertia system with backlash are proposed. The proposed methods utilize load-side encoder information effectively. Simulation and experimental results demonstrate the advantages of proposed methods quantitatively.**

***Index Terms*—Backlash, Two-inertia system, Joint torque, Load-side encoder, Disturbance observer**

I. INTRODUCTION

Precise joint torque control is highly required these days because it makes many things possible such as assembling by industrial robots, working safely in human living environments by welfare robots. These tasks are difficult to be accomplished by position control. Joint torque control can also improve backdrivability, which is an essential characteristic in wearable robots [1], [2].

The purpose of this research is to develop a precise joint torque control method for a two-inertia system. The precise joint torque control method is proposed considering plants' resonant characteristics and nonlinearities of transmission mechanisms.

A two-inertia system is widely studied because it is a general model and it represents resonant characteristics, which degrade control performance severely [3], [4], [5]. A two-inertia system consists of the drive side, the low stiffness transmission mechanism, and the load side. Transmission mechanisms such as gears and ball screws are not only low stiff but also they have nonlinearities such as backlash [6]. These undesirable elements deteriorate precision at the load side.

As the cost of encoders are lowering and the resolution is improving in the industry, the number of devices with load-side encoder is increasing aiming at higher precision at the load side. However, it is hard to say that research on control methods using load-side information is sufficiently conducted. More cost reduction in high resolution encoders will produce higher demands on novel control methods using load-side information effectively.

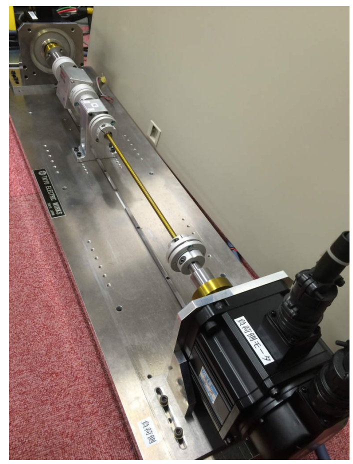

Fig. 1. Outlook of a two-inertia system motor bench.

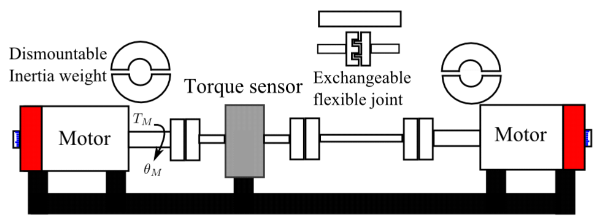

Fig. 2. Structure of a two-inertia system motor bench.

Our group has proposed a joint torque control method using load-side information [7]. Our research shows the advantages of the proposed joint torque control method by simulations and experiments. However, as for nonlinear compensation, which is one of the advantages of the proposed method, an analysis is limited to simulation-based one.

In this paper, effectiveness of nonlinear compensation is experimentally verified by using a setup which can be modelled as a two-inertia system with backlash. Moreover, based on the experimental results, a novel nonlinear compensation method is proposed and verified by experiments.

Also, a novel load-side torque control method is proposed

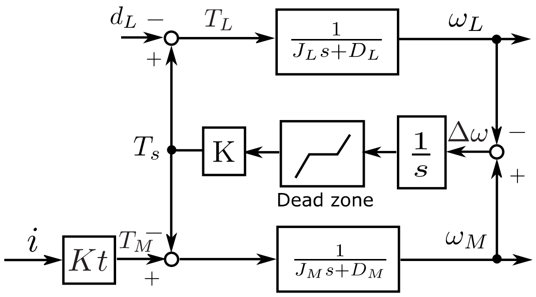

Fig. 3. Block diagram of a two-inertia system motor bench.

by applying a load-side disturbance observer to the proposed joint torque control method. The load-side torque control method is robust against the load-side disturbance.

This paper is organized as follows. An experimental setup is introduced and modelled in Section II. In Section III, proposed methods are explained in detail. In Section IV and V, performance of the proposed methods are quantitatively analyzed in simulations and experiments. Based on the experimental results, a novel nonlinear compensation model is proposed and analyzed experimentally in Section VI. Finally conclusions are given in Section VII.

II. Experimental Setup

A. Hardware

A motor bench with 20 bit high resolution encoders is used as a two-inertia system setup. Outlook and a schematic of the setup are shown in Fig. 1 and 2, respectively. To imitate a device with a low resonance mode, a low stiff joint can be inserted between two motors. Moreover, by replacing a flexible coupling with a gear coupling, backlash can be added and removed. Equipped high bandwidth torque sensor makes it possible to compare measured torque and estimated torque.

B. Modelling

A block diagram of a two-inertia model of the setup is shown in Fig. 3. Let inertia moment, viscosity, torsional rigidity, torque, and angular velocity be J, D, K, T, ω, respectively. Subscripts M and L indicate Motor side and Load side. Also, Joint torque, torsional angular velocity, motor current, and torque constant are indicated as $T_s, \Delta\omega, i, K_t$.

Generally, plants include various nonlinearities such as backlash [6]. In this paper, backlash is modelled as dead zone as shown in Fig. 3.

Frequency characteristics of the setup from the motor current to the drive-side angle and the load-side angle are shown in Fig. 4 and 5. These figures show that the setup can be modelled as a two-inertia system whose antiresonance frequency is 57 Hz and resonance frequency is 71 Hz. A fitted model is indicated in blue solid line while FRF measurement result is in red dashed line. Parameters identified by fitting are shown in Tab. 1.

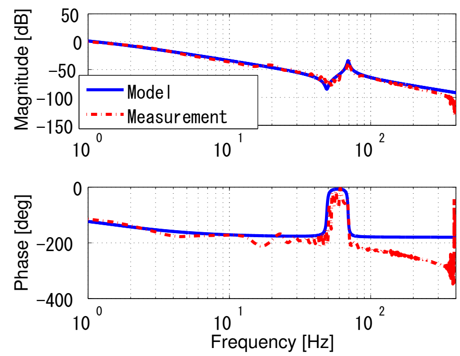

Fig. 4. Frequency responses from the drive-side input current to the drive side angle.

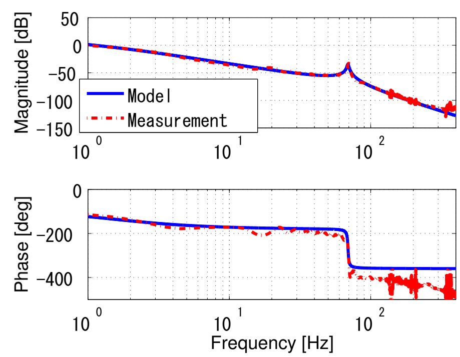

Fig. 5. Frequency responses from the drive-side input current to the load side angle.

C. Backlash identification

For backlash identification, drive-side velocity control is implemented. As shown in (1), backlash can be calculated by integrating the torsional angular velocity between t_1, when the load separates from the drive side and t_2, when the load contacts the drive side again [8], [9]. Let dead zone width be $\pm\epsilon$.

$$2\epsilon = \left| \int_{t_1}^{t_2} (\omega_M - \omega_L) \right| \quad (1)$$

In the experiments, dead zone width is calculated by not integrating the torsional angular velocity but using the angles at t_1, t_2 obtained by the encoders on drive and load sides. Fig. 6 shows a part of the identification experiments. Averaging the results leads to $\epsilon = 6.0$ mrad.

III. Proposed Methods

A. Outline

Based on a trend expanding the use of load-side encoders in the industry, a joint torque control method is proposed for a two-inertia system with a load-side encoder. Utilizing both drive and load side information makes torsional angular velocity control possible, and this can make precise joint torque control possible. Moreover, torsional angular velocity

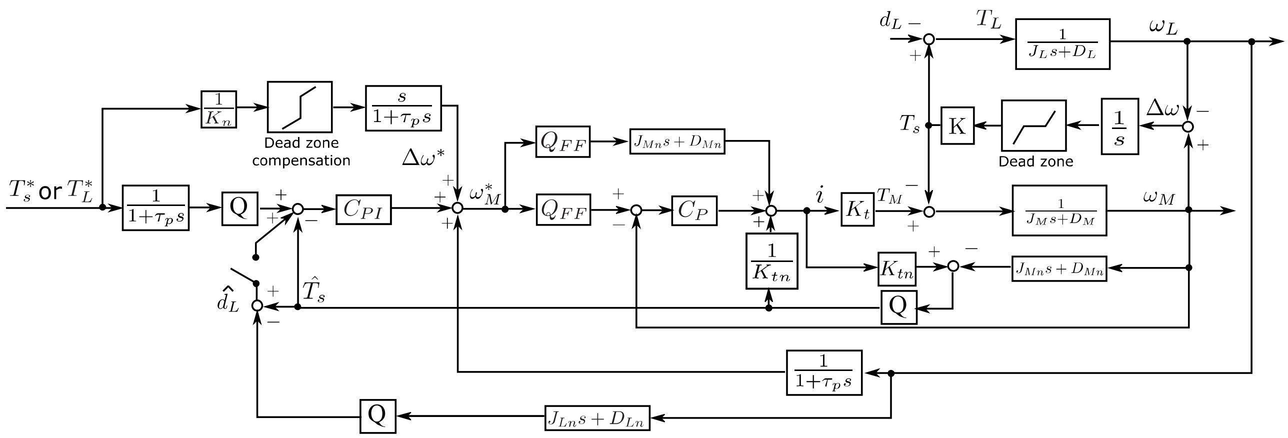

Fig. 7. Block diagram of the proposed methods.

TABLE I
PARAMETERS OF THE TWO-INERTIA SYSTEM MOTOR BENCH.

Motor-side moment of inertia J_M	1.05e-3	kgm^2
Motor-side viscosity friction coefficient D_M	1.00e-2	Nms/rad
Torsional rigidity coefficient K	99.0	Nm/rad
Load-side moment of inertia J_L	1.05e-3	kgm^2
Load-side viscosity friction coefficient D_L	1.00e-2	Nms/rad

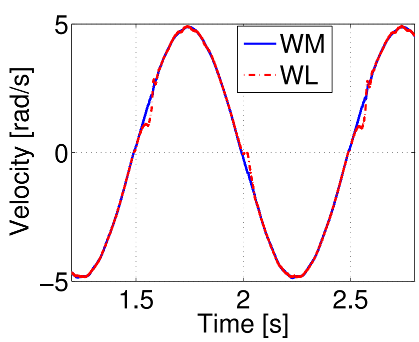

Fig. 6. Identification of backlash.

control enables us to design feed forward (FF) controller considering nonlinear elements at transmission mechanisms such as backlash and nonlinear springs etc., which are often ignored in conventional joint torque control methods. The proposed method does not need a torque sensor, which has the disadvantages such as lowering rigidity and high cost etc.

Fig. 7 shows a block diagram of proposed methods: a joint torque control method and a load-side torque control method. When a load-side disturbance observer (LDOB) is implemented by feed backing estimated load-side disturbance $\hat{d}_L$ as shown in Fig. 7, the joint torque control method becomes the load-side torque control method, which is robust against the load-side disturbance. The symbols in the block diagram indicate the following: C_P: a P controller of the drive-side angular velocity, C_{PI}: a PI controller of the joint torque, $\hat{T}_s$: the joint torque estimated by a reaction force observer (RFOB), $\hat{d}_L$: the load-side torque estimated by a LDOB, Q: low pass filter (LPF) of DOB, Q_{RFOB}: LPF of RFOB, Q_{FF}: the 1st order LPF to make an angular velocity FF controller proper, τ_p: time constant of pseudo differential. Subscripts $_n$ denote nominal values and superscripts * mean reference values.

B. Joint torque control

The proposed joint torque control method can be divided into three parts. The first part is a drive-side velocity control part, the second part is a joint torque FF control part which generates torsional angular velocity reference value from joint torque reference value, and the third part is a joint torque FB control part using the joint torque estimated by RFOB.

The proposed method controls the joint torque by controlling the torsional angular velocity. For torsional angular velocity control, collocated drive-side angular velocity is controlled and then combined with the load-side angular velocity obtained by a load-side encoder. Here, from Fig. 7 the torsional angular velocity $\Delta\omega$ is obtained as (2).

$$\Delta\omega = \omega_M - \omega_L \tag{2}$$

Therefore, the reference value of the drive-side angular velocity can be generated as (3) by using the reference value of the torsional angular velocity and the load-side angular velocity.

$$\omega_M^* = \Delta\omega^* + \omega_L \tag{3}$$

The drive-side angular velocity is controlled by DOB and a P controller. A drive-side angular velocity FF controller is also applied to achieve a high control bandwidth. A higher control bandwidth of the inner loop control improves a response of an outer loop. The drive-side angular velocity FF controller is implemented as $(J_{Mn}s + D_{Mn})$ on the assumption that the reaction joint torque is decoupled by DOB. Then the first order LPF Q_{FF} is applied to make $(J_{Mn}s + D_{Mn})$ proper.

The joint torque FF control part generates the reference value of the drive-side angular velocity from the reference value of the joint torque. Considering an inverse model of the transfer function from $\Delta\omega$ to T_s shown in Fig. 3, the

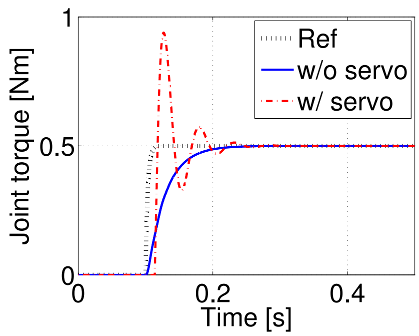

Fig. 8. Step responses of the joint torque with and without load-side servo.

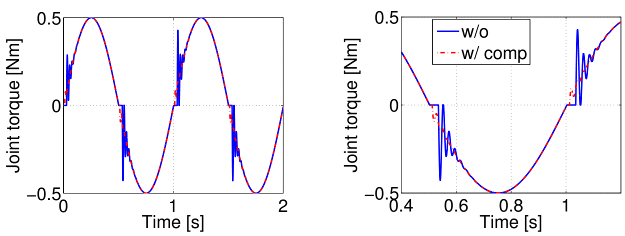

(a) Sinusoidal response of the joint torque

(b) Zoom of the left figure

Fig. 9. Comparison between with and without backlash compensation.

reference value of the drive-side angular velocity is generated by using the reciprocal of the torsional rigidity, the inverse model of nonlinear elements, and the derivative. The derivative is implemented as pseudo differential with time constant τ_p. In this paper, backlash is modelled as dead zone. Therefore, the inverse model of dead zone is applied for nonlinear compensation.

The joint torque FB control part controls the estimated joint torque with a PI controller. The PI controller is designed by the pole placement to the plant, $T_s = \frac{k}{s}\Delta\omega$. The PI control enables us to control joint torque without state steady error.

C. Load-side torque control

When the load-side disturbance is large, a load-side torque control method should be implemented. Applying LDOB, which estimates the load-side disturbance d_L by using load-side encoder information, to the proposed joint torque control method makes load-side torque control possible. Here, load-side torque $T_L$is a torque which directly drives a load. It consists of the joint torque and the load-side disturbance. The load-side torque control method is implemented by feed backing $\hat{d}_L$ as shown in Fig. 7.

IV. Simulations

A. Joint torque control

The model used in simulations is the identified two-inertia system model whose parameters are shown in Tab. 1. For simplicity, the plant model has neither nonlinear elements nor modelling errors unless it is clearly stated.

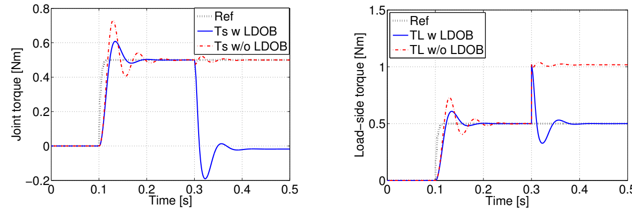

(a) Joint torque responses

(b) Load-side toque responses

Fig. 10. Comparison between with and without LDOB.

The drive-side angular velocity P controller and DOB are designed such that their control bandwidth become as high as possible considering the stable margin. The cut-off frequency of RFOB are set as 50 Hz. The PI controller for the joint torque is designed by pole placement.

Step responses of the joint torque are shown in Fig. 8. In the experiments explained in the next section, the load-side motor is controlled and fixed by a PID position controller to prevent the motor from rotating too fast. Black dotted line indicates a step reference with low pass filter whose cut off frequency is 50 Hz, while blue solid line is a joint torque response without load-side servo, red dashed line is one with servo. With servo control, the response has larger vibration because it works as a load-side disturbance. Please note that all simulation and experimental results below are the results with load-side servo.

B. Backlash compensation

Dead zone width used in simulations is ±6.0 mrad which is identified experimentally in Section II–C. Initial position is in the middle of dead zone. Since backlash has an effect at the reversal points, sinusoidal responses are shown in Fig. 9(a) and (b). Without backlash compensation, the response sticks to 0 Nm at the reversal points, and then after the dead zone width it shows large vibration by collision between the motor side and the load side. The simulation result clearly shows that the proposed backlash compensation method improves the response.

C. Load-side torque control

Fig. 10(a) and 10(b) show the comparison of both the joint torque and the load-side torque responses between the joint torque control method and the load-side torque control method. Step disturbance is input at 0.30 s at the load side. In joint torque control indicated in red dashed line, joint torque is controlled even with the load-side step disturbance. Therefore, load-side torque cannot be controlled. On the other hand, load-side torque control indicated in blue solid line can control the load-side torque robustly by considering the load-side disturbance.

V. Experiments

The conditions in the experiments are the same as those in the simulations. Controllers are discretized by Tustin conversion whose sampling frequency is 2 kHz.

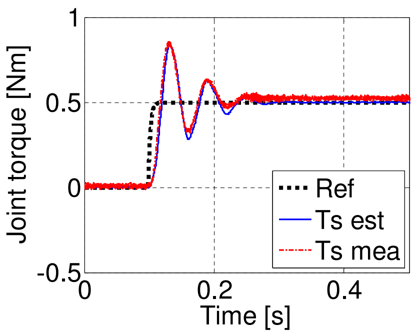

Fig. 11. Step response of the joint torque.

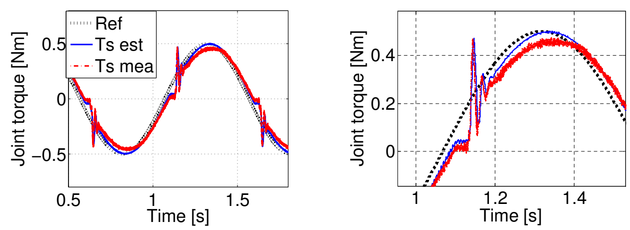

(a) Sinusoidal response of the joint torque

(b) Zoom of the left figure

Fig. 12. Joint torque response with backlash.

A. Joint torque control

Experimental results of the joint torque step responses are shown in Fig. 11. Black dotted line indicates step reference, while blue solid line indicates estimated value, red dashed line indicates measured torque. Experimental results are well similar to the simulation result shown in Fig. 8 with servo.

B. Backlash compensation

Fig. 12(a) and (b) show the responses of joint torque with backlash. The deterioration by backlash is clearly seen. Also, the results show that the estimation of the joint torque is highly precise.

The responses with backlash compensation based on the inverse dead zone model is shown in Fig. 13(a) and (b). Fig. 14(a) shows the current in this response. In this experiment, cut off frequency of pseudo differential in joint torque FF controller is lowered to 10 Hz to avoid exceeding maximum motor torque. Fig. 13(a) shows that it can suppress the maximum amplitude of the response after the reversal points compared to Fig. 12(a), but it also produces a spike at the compensation timing. This is caused by differential of the inverse dead zone model in FF controller. Therefore, the compensation model needs to be improved such that the differential of the model becomes gentle and smooth. A novel compensation model is proposed based on this result in Section VI.

C. Load-side torque control

In the setup, since load-side torque cannot be measured, a joint torque response is shown and compared to the simulation

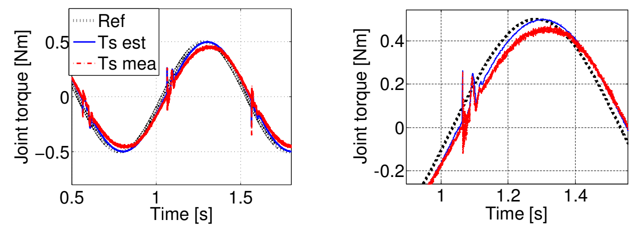

(a) Sinusoidal response of the joint torque

(b) Zoom of the left figure

Fig. 13. Experimental comparison between with and without backlash compensation.

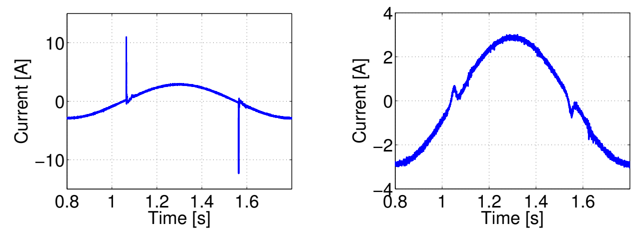

(a) Inverse dead zone model

(b) Proposed model

Fig. 14. Comparison of the current responses in backlash compensation.

result. Fig. 15(a) and (b) show the comparison of the joint torque responses between the joint torque control method and the load-side torque control method. Step disturbance is input at 0.25 s at the load side. These results coincide with the result shown in Fig. 10(a). Since they show well similar results, it can be inferred that the load-side torque is properly controlled. The vibration in Fig. 15(b) is caused by the load-side servo control, which works as the load-side disturbance.

VI. Backlash Compensation Based on Sigmoid Function Model

A. Sigmoid function

Aiming at a better response and smaller maximum motor torque, a novel backlash compensation model is proposed using sigmoid function expressed as (4). Here, K_{sig} is a total gain and a is a gain determining the similarity to the inverse dead zone model as shown in Fig. 16(a).

$$\zeta(x) = K_{sig}\left(\frac{1}{1+e^{-ax}} - \frac{1}{2}\right) \tag{4}$$

As shown in Fig. 16(b), tangential lines at the points $-x_1$ and x_1 at which the slopes of sigmoid function are 1 are drawn. Then by defining a new model as (5), it becomes a smoothed inverse dead zone model.

$$\zeta^{'}(x) = \begin{cases} x + x_1 + \zeta(-x_1) & (x < -x_1) \\ \zeta(x) & (-x_1 \le x \le x_1) \\ x - x_1 + \zeta(x_1) & (x > x_1) \end{cases} \tag{5}$$

Since pseudo differential of this smoothed model becomes FF output, smaller maximum motor torque is required. The design parameters are two, K_{sig} and a. After a is tuned, K_{sig} can

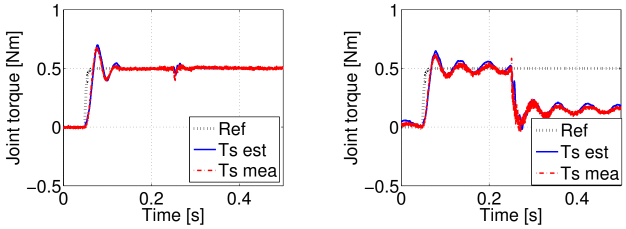

(a) Joint torque control (b) Load-side torque control

Fig. 15. Comparison of joint torque response between with and without LDOB.

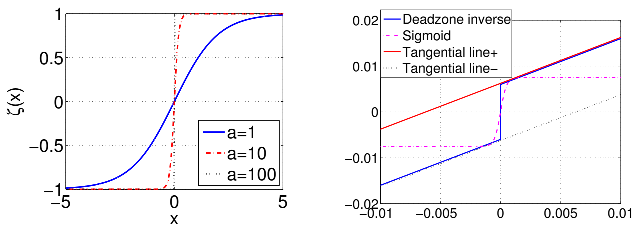

(a) Sigmoid function with variable a (b) Inverse model of dead zone and the proposed model.

Fig. 16. Backlash compensation models.

be tuned by comparing the intercepts of tangential lines and the identified dead zone width.

The comparison of the joint torque response between with and without backlash compensation based on the proposed model is shown in Fig. 17 and Fig. 18. Here, K_{sig} and a are tuned as 0.050 and 5000, respectively. Cut off frequency of pseudo differential in the joint torque FF controller is 10 Hz. Clear improvement can be seen and there is no spike. A current response is shown in Fig. 14(b). The new compensation method decreases the required maximum motor torque drastically.

VII. Conclusion

Considering the industrial trend that the number of the devices with load-side encoder is increasing, the joint torque control method and the load-side torque control method using a load-side encoder are proposed and their effectiveness are verified by simulations and experiments. Based on the experimental results that the inverse dead zone based backlash compensation method produced a spike at the compensation timing and large peak current is required, a novel backlash compensation model are proposed and it shows better performance.

Backlash compensation method using load-side encoder information more effectively will be studied in the near future.

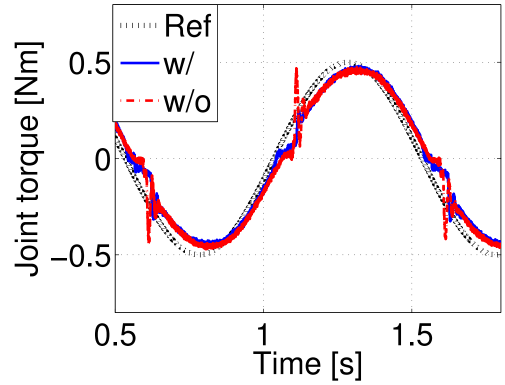

Fig. 17. Comparison of the sinusoidal response of the joint torque with and without the proposed backlash compensation.

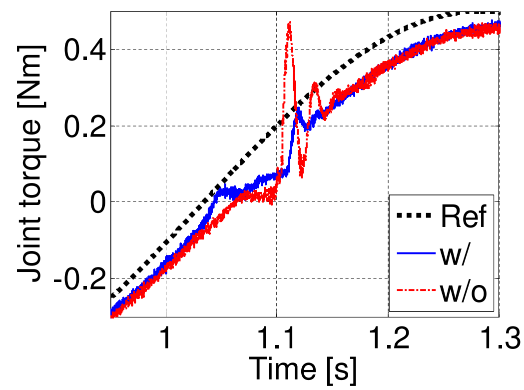

Fig. 18. Zoom of Fig. 17.

References

[1] K. Kong, J. Bae, and M. Tomizuka: "A Compact Rotary Series Elastic Actuator for Human Assistive Systems", *IEEE Trans. on Mechatronics*, Vol. 17, No. 2, (2012).

[2] N. Paine, S. Oh, and L. Sentis: "Design and Control Considerations for High-Performance Series Elastic Actuator", *IEEE Trans. on Mechatronics*, Vol. 19, No. 3, (2014).

[3] K. Szabat and T. Orlowska-Kowalska: "Vibration Suppression in a Two-Mass Drive System Using PI Speed Controller and Additional Feedbacks–Comparative Study", *IEEE Trans. Ind. Electron*, Vol. 54, No. 2, pp. 1193–1206, (2007).

[4] K. Yuki, T. Murakami, and K. Ohnishi: "Vibration Control of 2 Mass Resonant System by Resonance Ratio Control", *Industrial Electronics Society Annual Conference (IECON-1993)*, pp. 2009–2014, (1993).

[5] Y. Hori, H. Iseki, and K. Sugiura: "Basic consideration of vibration suppression and disturbance rejection control of multi-inertia system using SFLAC (state feedback and load acceleration control)", *IEEE Trans. Ind. Applications*, Vol. 30, No. 4, pp. 889–896, (1994).

[6] M. Iwasaki, M. Kainuma, M. Yamamoto and Y. Okitsu: "Compensation by Exact Linearization Method for Nonlinear Components in Positioning Device with Harmonic Drive Gearings", *Journal of JSPE*, Vol. 78, No. 7, pp. 624–630, (2012).

[7] S. Yamada, K. Inukai, H. Fujimoto, K. Omata, Y. Takeda, and S. Makinouchi: "Joinrt torque control for two-inertia system with encoders on drive and load sides", *Proc. of the 13th IEEE Int. Conf. on Industrial Informatics (INDIN)*, pp. 396–401, (2015).

[8] S. Villwock, and M. Pacas: "Time-Domain Identification Method for Detecting Mechanical Backlash in Electrical Drives", *IEEE Trans. Ind. Electron*, Vol. 56, No. 2, (2012).

[9] K. Yuki, T. Murakami, and K. Ohnishi: "Study of on-line backlash identification for PMSM servo system", *Proc. of the 38h annual conference on IEEE Industrial Electronics Society (IECON)*, pp. 2036–2042, (2012).